Development of Smart Battery Cells through Sensor Instrumentation and In-Vehicle Power Line Communication

Timothy A. Vincent
Cell Instrumentation Team, WMG
University of Warwick
Coventry, United Kingdom
T.A.Vincent@Warwick.ac.uk

James Marco
Cell Instrumentation Team, WMG
University of Warwick
Coventry, United Kingdom
James.Marco@Warwick.ac.uk

***Abstract*— Smart cells, instrumented with miniature sensors, can help meet both the consumer and regulatory demands for the battery packs of next-generation of electric vehicles (EVs). Currently, adding sensors to battery packs entails increasing vehicle weight and complexity with the associated wiring loom expansion.**

In this work, we demonstrate sensors for voltage, current and temperature can be installed on cylindrical cells (21700 format) and connected to a data logger via power line communication (PLC). We achieved zero error rate with our laboratory setup, and transfer times of < 40 ms (relative to dedicated wired connection). This reliable PLC method (max. data transfer rate 115 kbps) was sufficient for logging cell data and can operate over a wide DC voltage range (e.g. target 10 to 60 V typical in an EV). Our initial experiments highlight the lack of understanding of the performance of a cell during its lifetime in an EV, where temperature gradients were observed between the terminals (0.2 °C with a peak increase of +0.6 °C, discharge rate of 0.5 C).

Keywords— Cell Instrumentation, temperature sensing, real-time dynamic measurements, vehicle PLC.

I. INTRODUCTION

The rapid growth in the worldwide EV market (3 million EVs on the road in 2018, double the 2016 total [1]) has invoked demand for low-cost Lithium-ion (Li-ion) battery cells. To maintain this EV growth rate, adoption barriers (e.g. range anxiety and charging times [2]) must be overcome. Next-generation Li-ion cells must offer high density and long lifetimes (current lifetime order of 3 to 5 years [3]) to achieve these targets.

The lack of knowledge regarding the health (e.g. rate of aging) of an individual cell in a battery module or complete pack currently limits the maximum achievable performance, where blanket and conservative limits (i.e. rate of charging and discharging) are often applied. We aim to provide this information, through the development of smart cells, where each cell can be instrumented with a variety of sensors (e.g. temperature, current, voltage) and controlled (e.g. disconnected from the pack when necessary).This will reduce the need to over-engineer the pack, saving weight, volume and cost. Data from these sensors can be given to computational models within the vehicle's battery management system (BMS) to optimise the performance of the pack. In this work we demonstrate a proof-of-concept system to show that PLC can be used to provide the crucial link between the sensors (within smart cells) and the central BMS.

This work is funded in-part from the ESPRC Prosperity Partnership grant, R004927.

978-1-7281-4816-8/20/$31.00 ©2020 IEEE

PLC systems for in-vehicle use have previously been reported [4][5], however these systems are used outside of the battery pack, to communicate between peripherals inside the vehicle. PLC has been proven to serve as a replacement for Ethernet connections inside a vehicle, serving accessories to the vehicle, such as cameras and media systems [4]. It has not yet been proven to operate with real-time, safety critical applications. Communicating via the DC bus bars inside a pack presents additional challenges; varying DC voltage levels, the need to prioritise message traffic, reliability in a harsh environment and connecting networks with tens of nodes. We aim to expand upon these systems, through development of a PLC network, addressing these challenges, for use in an EV's battery pack. We use our novel sensors to provide data related to calculating the state of health of a cell.

This paper is structured as follows: Our motivation for developing a PLC and sensor system; the methodology for our PLC experiments describing our test scenarios; the results and findings from our experimental data followed by the conclusions from our trials and our future work.

II. MOTIVATION

In EVs, the task of predicting and monitoring the health of cells inside a pack is performed within the BMS. With the current design of EV batteries, the BMS relies on a subset of temperature (Nissan leaf 3 sensors [6], in general rarely above 16 [7]) and voltage sensors to measure the health of the pack. Single sensors are used to monitor an entire module (containing tens of cells). Hotspots can occur in cells - surface temperature is not truly representative of the core (10 °C difference possible [8]). Improving performance of cells is important, with demand for faster charging EVs to infiltrate the combustion engine market for long distance transport. Stringent safety regulations will likely need advanced warning of hazardous situations (e.g. 5 minute alert to passengers) [9]. Additional sensors will be required within EVs, but without adding extra weight, cost n complicated wiring harnesses.

PLC offers an ideal solution to reducing the wiring harness within a pack, while allowing an unrestricted number of instrumented cells. Bi-directional communication is typical, permitting two-way communication between cells and the BMS (e.g. disconnect malfunctioning cells). We propose the PLC system interfaces to the BMS via a CAN bus, enabling perhaps independent networks in each battery module. Previously, techniques such as wireless transmission have been considered [10]. In the automotive industry this raises

concerns regarding reliability / security [11]. These systems are complex and bi-directional communication cannot be assumed to be trivial. Integrating an antenna within a battery module or pack is difficult, considering the physical space needed, pack materials and robustness.

The PLC network will be adaptable to operate at the DC voltage range of the pack (not fixed). We target reliable operation regardless of module configuration (while maintaining operation in the case of a cell failure). The system must retain functionality when the module is removed from the pack (e.g. for second-life servicing). A module, containing for example 16 lithium ion cells, (such as in the Renault Zoe, containing 12 modules), can vary between approximately 43 V and 70 V (nominal cell voltage of 3.75 V) [12].

III. METHODOLOGY

The proof-of-concept PLC system (block-diagram Fig. 1) comprises: Three cylindrical cells (21700 40T, 4000 mAh capacity, charged to 50 % state of charge, Samsung SDI, South Korea), two microcontrollers (Teensy 3.2, PJRC, USA) and interface circuitry for our cell sensors and two PLC transceivers (SIG60, Yamar Electronics Ltd, Israel).

The SIG60 modem, operational diagram shown in Fig.2 [13], was chosen for its operation at low voltage DC levels (suitable for low voltage laboratory testing and worst case scenarios, if cells fail in a module). The SIG60 allows for up to 16 different frequency pairs on each power line, allowing separate networks to operate concurrently. Thus, it is proposed a separate frequency pair is assigned to each module inside a vehicle. For this work, the frequency pair of operation was set to F0 5.5 MHz and F1 6.5 MHz (range selected for robust link while above the range of frequencies where impedance of the cell causes interference). Data from one instrumented cell is collected. Data transfer rates required are in the order of 100s of kbps, (115 kbps maximum possible with this configuration) to allow changes in cell temperature to be monitored in real-time. In this application, higher data transfer rates are needed than found in narrowband PLC modems, where other devices are limited to low kbps (e.g. 2.4 kbps [14]) transfer rates.

The power-lines within a battery module offer greater challenges (harsh environment, large temperature variation) compared to the DC rails in a vehicle's cabin. Frequency shift keying (FSK) is preferred over phase shifting keying (PSK); the impedance of the cells will vary over their lifetime and battery state of charge (SOC) and varies greatly depending on the transmission frequency (this effect is advantageous for studying cell health via Electrochemical Impedance Spectroscopy [15]). The SIG60 modems were selected to offer robust communication regardless of cell age.

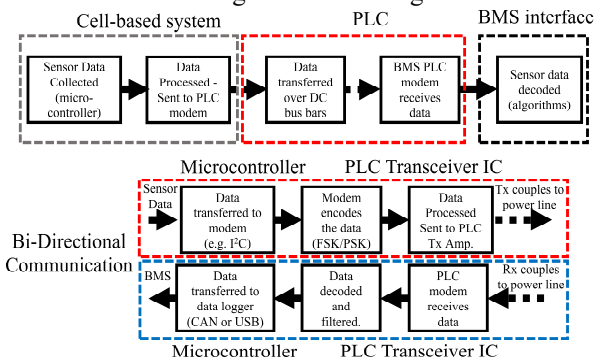

Fig. 1. Block diagram showing components in cell PLC instrumentation system and operation of bi-directional communication.

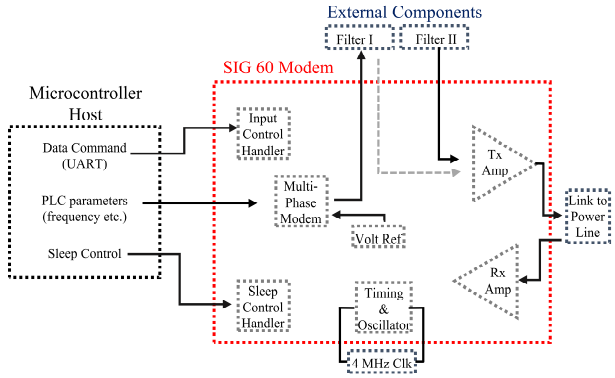

Fig. 2. Operation of Yamar Electronics SIG60 PLC modem with host microcontroller.

It is important to analyse trends in temperature response in real-time to aid detection of thermal runway events. A module of cells is ideal for safe prototyping and laboratory testing (e.g. this PLC system is currently capable of operating at a voltage range of 10 to 36 V). The setup is designed to operate at low DC voltages for different configurations in a module (selected PLC modem and microcontroller operate at nominal 3.3V).

Measurements of current, temperature and cell voltage are considered pertinent to model cell behaviour. In this application, these sensors must be resilient to the harsh environment experienced inside a battery pack (electrolyte leakage possible), and capable of withstanding wide temperature fluctuations.

An array of thermistors enables a map of the cell temperature to be created. We have developed a flexible (polyimide substrate) PCB to hold the sensors inside the cell. In this work the sensors are placed externally on the cell surface, with the cell placed in a custom designed and manufactured cell holder, as shown in Fig. 3 (a). The custom holder allows the terminals of the cell to be accessible (small pins used for electrical contact), and permits space for cells to be internally instrumented through the negative cap. Thermistors are preferred to measure an array of temperatures, as the usual sensors used in modules (thermocouples) are suitable for single measurements only (requiring a cold junction, and not possible to combine into an array of sensors).

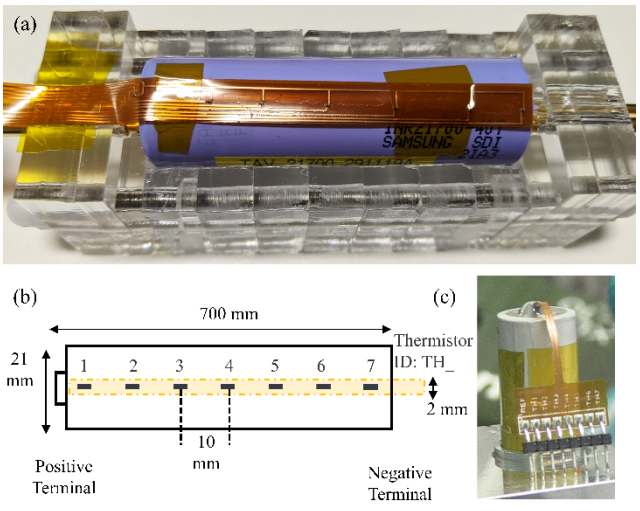

Fig. 3. Cylindrical cell instrumented with thermistor temperature sensors; (a) thermistor strip installed externally; (b) layout of inserting strip into core of cell and (c) completed assembly process of internally instrumented cell.

The flexible PCB design allows the temperature to be monitored at 10 mm sections along the surface of the cell. 0402 size thermistors are mounted on the PCB, layout shown in Fig. 3 (b). The assembled PCB is coated with a uniform polymer layer (Parylene C, ~ 15 µm thick) to prevent damage from the electrolyte inside the cell. Fig. 3 (c) shows an instrumented cell, during the assembly process when inserting the flexible PCB into the core of the cell.

A Hall Effect sensor was selected for current measurement (MAX31850K, Maxim Integrated, USA). This method allows a wide range of current to be detected (10s of mA range to 5 A), without danger of external heating (shunt resistor, which could also dominate the impedance of the cell). In this prototype design, the voltage is measured across the power line. In future work, a reference electrode is proposed to measure voltages at the cathode and anode, adding further refinement and accuracy to the experimental set-up.

The use of a microcontroller (interface between sensors and PLC modem) removes the limit on the number and type of sensors it is possible to install in the cell (SIG60 offers only UART interface, which is used to communicate with the microcontroller). The Teensy 3.2 offers ADC, I2C, SPI interfaces (for this work, 9 ADC channels are used). The complete transmission system (microcontroller, sensor interface boards, PLC modem) are powered off the same power line.

For laboratory measurements, 10 Hz data logging rate was considered suitable to track changes in cell temperature. For monitoring of a module (for example containing > 8 cells) it is proposed the data rate is reduced to 1 Hz, where the microcontroller can be used to perform initial signal processing. Measurements of voltage, current and temperature (12-bit ADC) were taken at 100 Hz, then averaged prior to output via PLC. A string (length 488 bits per cell) is transferred over the power line (to computer via USB connection), containing the data in raw format. At the occurrence of a sudden increase in temperature (e.g. exceeding defined limit), the data rate can be increased/prioritised to log the onset of this temperature rise.

The PLC method was verified under four cell discharging scenarios (Sn):

- (S1) baseline conditions, minimal current drawn (powering PLC modems/interface circuitry only);
- (S2) high resistance wire connection (LED strip, 2m length, discharging rate ~0.166 C);
- (S3) similar discharge rate (0.2 C) but with resistive load;
- (S4) higher discharge rate (~0.5 C).

In each of these conditions, data were logged from a direct USB/serial connection to the microcontroller acquiring data from the sensors ('direct connection') and secondly a microcontroller collecting data from the PLC modem receiver ('PLC connection'). The success of the transfer was verified (direct vs PLC connection) in terms of bit error rate (BER). The transmission speed was verified by subtracting the timestamp of the data logged on the computer via each method.

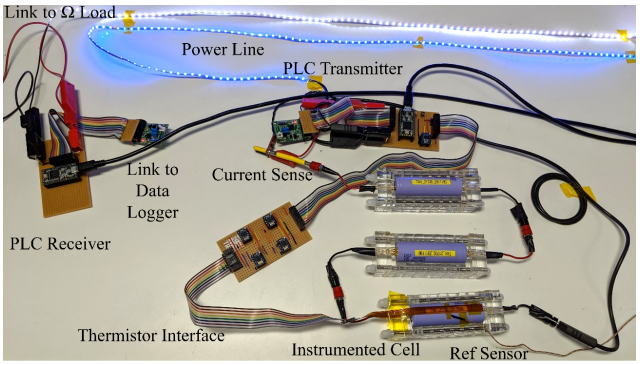

Fig. 4. Photograph of laboratory setup configured for scenario S1.

IV. Results and Discussion

The first connection scenario was used as a baseline prior to any adjustment of load or power line configuration, where a short connection (< 0.3 m) was inserted as the power line. Data were logged continuously from the instrumented cell sensors throughout the experiment. Fig. 4 shows a photograph of the system configured as per S1. Data shown in Fig. 5, demonstrates acquisition of data from the thermistor PCB (PLC connection); here data from the cell terminals and central thermistor are plotted. A 3 minute period was allowed in baseline conditions, scenario (S1), before switching to (S2) for 15 minutes. A period of ~ 20 minutes settling was allowed at the end (returning to S1).

Voltage and current data were logged during the experiment, shown in Fig. 6 (a). The additional time taken to receive the PLC data (relative to the direct USB connection) is shown in Fig. 6 (b). On average, each data string was delayed by circa 38 ms (total number of ~21.6 k messages). During a comparison of the raw data received from each connection, no bit errors were detected.

Thermistor data demonstrated a minor increase in cell surface temperature (environmental temperature ~21.7 °C to peak temperature of 22.1 °C). The positive terminal shows ~+0.1 °C offset compared to negative terminal for this experiment. This effect has been previously reported [16], although it is magnified at higher charging rates.

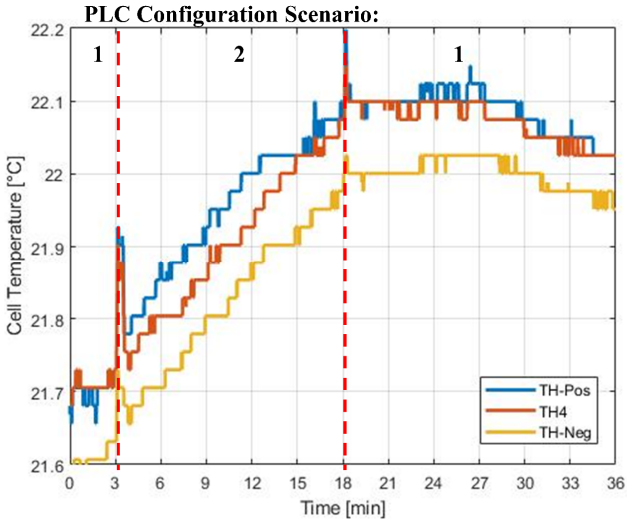

Fig. 5. Thermistor measurements recorded along surface of cell; Three data plots shown – thermistors located at positive and negative terminals and centre of cell (data recorded via PLC). Scenarios 1 and 2 tested.

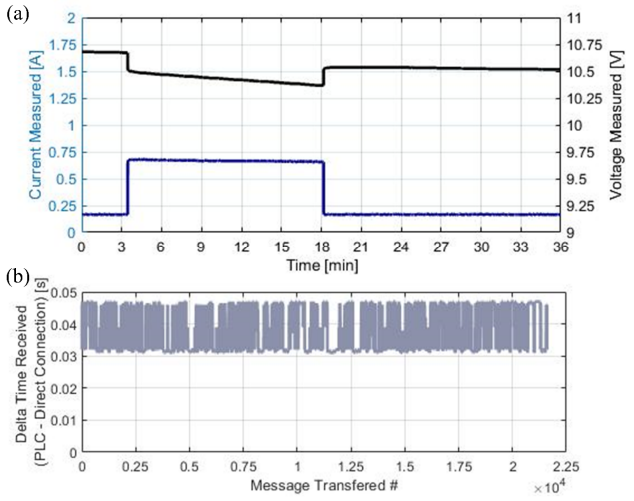

Fig. 6. (a) Voltage and current data recorded via PLC connection. Low current load (~0.7 A maximum), data logged via PLC. (b) Time between messages received via direct and PLC connections. Scenarios 1 and 2 tested.

The cells were not actively cooled during this work, and (for safety reasons) were operated below their maximum discharge rate. The PLC link was proven to be unaffected by the LED power line, and all data was successfully transferred with acceptable time delay (< 100 ms delay).

Scenarios S3 and S4 were tested using resistive loads to apply discharge rates of 0.2 and 0.5 C (10 and 6 Ω loads, respectively). Data shown in Fig. 7 shows the thermistor data (terminals and centre of cell), for when the cell was subjected to the following regime: 1 min baseline S1; 3 min S3 (0.2C discharge); 4 min S4 (0.5C discharge) and 10 min return to baseline (S1).

A similar temperature gradient is observed; the positive terminal is ~+0.1 °C higher temperature compared to the negative, particularly at peak load. The cell does not cool back to baseline during the course of the experiment, although no cooling was implemented. This work focuses on the ability of the PLC system to transfer data not on cell operation).

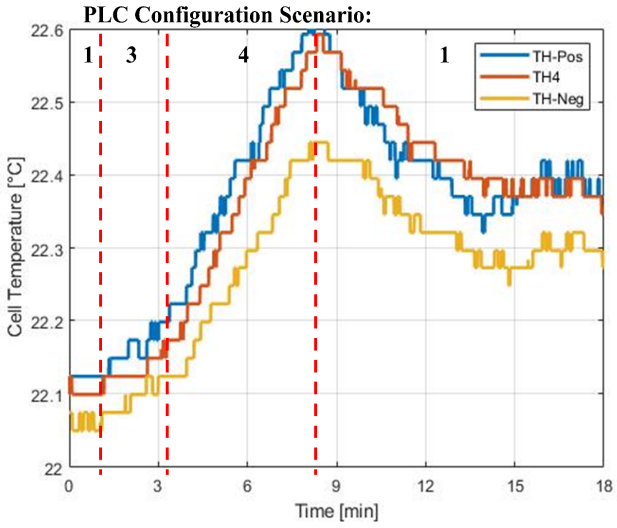

Fig. 7. Temperature data recorded (positive, negative terminals and centre location thermistor data shown) of surface of 21700 cell subjected to current load of 0.8 and 1.7 A (scenarios 1, 3 and 4 tested) Temperature graident visible: positive terminal highest temperature; central TH4 data lower temperature; lowest temperature for sensor located on negative terminal.

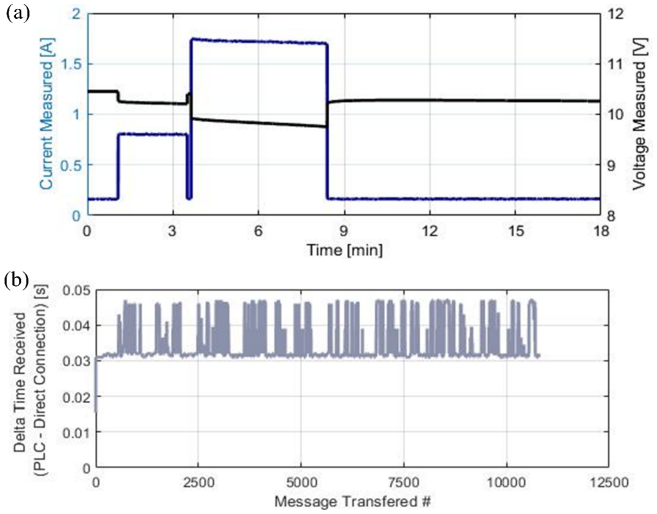

Fig. 8. (a) Voltage and current data recorded via PLC system, when cells discharged at 0.2 and 0.5 C rate. (b) Direct vs PLC connection delta time to receive given message. Scenarios 1, 3 and 4 tested.

Data were recorded for the current load and voltage of the cells during the experiment, shown in Fig. 8 (a). The peak discharge rate (~1.7 A) initiated a peak change of ~+0.6 °C from the baseline temperature. The peak temperature is reached after the resistive load is removed (~1 min delay), demonstrating the need to internally instrument the cells, to provide faster warning of high temperatures.

Fig. 8 (b) demonstrates that across the ~12.5k messages transmitted, the delay between the direct and PLC connections was ~34 ms. Again the BER was zero, where it was found that all messages were received successfully and integrity preserved. The experiments serve as proof-of-concept that our PLC system can operate with a module to transmit sensor data between the acquisition point and a central logging system. From each cell, ~3.9 kB of data is transmitted per measurement period (10 Hz rate), highlighting the need for faster PLC data transfer rates considering the potentially high number of transmitting nodes, e.g. >16 cells in a module. The zero BER achieved in these experiments proves the robustness of the system in a laboratory setup.

V. Conclusions

Previously, PLC systems have been demonstrated for in-vehicle use, and we further this research demonstrating a system for use within a battery pack. Our novel sensors allow cells to be instrumented with temperature, voltage and current sensors, to provide important data regarding the cells health and performance to the BMS. Currently, the cells have been externally instrumented to verify the functionality of the PLC system at low DC voltage (~ 10 V), but in future work we aim to instrument the cells with an array of thermistor sensors (7 sensors in a 21700 cell, providing a 10 mm resolution map of core temperature). Together with our miniature PLC system, we aim to provide a cost efficient means to instrument our smart cells, and create batteries for the next generation EVs.

The PLC and module system was subjected to four discharge scenarios to demonstrate the resilience of the communication link to varying DC voltage and current supply; baseline conditions (0.1 A discharge), high resistance wire discharge (LED strip, 0.7 A discharge), resistive load (0.8 A discharge) and lower resistive load (1.7 A discharge).

Data were logged from the temperature, current and voltage sensors throughout. A zero BER was achieved, demonstrating the system was resilient to changes in power line quality and unaffected by resistive loads.

The external thermistors demonstrated the need for understanding the operation of a cell in a pack, where a temperature gradient (~16 %, 0.2 °C) was consistently observed between the positive and negative terminals of the cell (0.5 C rate, magnitude of gradient likely to be higher at nominal C rate). The temperature gradients observed are consistent with values previously reported in the literature, thus demonstrating our PLC system can successfully transferring temperature data to a central logging system, without influencing cell performance. The delayed response (~ 1 min) demonstrated the need to further our work instrumenting the cells internally, to provide an instant response to hotspots.

VI. Further work

We aim to further assess the resilience of the system with greater discharge loads, additional noise sources and greater voltage changes (operating between 60 V and 8 V). Future work also involves testing the PLC system with a module of cells in a temperature controlled environment, at higher discharge and charge rates. We aim to benchmark the Yamar modem against system-on-chip modems, which offer a complete solution to acquire data and transmit over a power line. We will analyse the robustness of the developed PLC systems considering injecting noise into the system (similar to that found in real-world EVs).

Our system has been shown to be function with a 3-series cell configuration. Our testing methodology will be extended to test a range of series/parallel configurations with a larger number of cells (e.g. 8 cells, 4-S-2-P). We will verify the system remains functional with a battery module with higher charge and discharge rates.

VII. Acknowledgements

EPSRC - This work is funded in-part from the Prosperity Partnership grant, R004927.

References

[1] J. Earl and M. J. Fell, “Electric vehicle manufacturers’ perceptions of the market potential for demand-side flexibility using electric vehicles in the United Kingdom,” Energy Policy, vol. 129, pp. 646–652, Jun. 2019.

[2] Q. Zhang et al., “Factors influencing the economics of public charging infrastructures for EV – A review,” Renew. Sustain. Energy Rev., vol. 94, pp. 500–509, Oct. 2018.

[3] E. Sarasketa-Zabala, E. Martinez-Laserna, M. Berecibar, I. Gandiaga, L. M. Rodriguez-Martinez, and I. Villarreal, “Realistic lifetime prediction approach for Li-ion batteries,” Appl. Energy, vol. 162, pp. 839–852, Jan. 2016.

[4] W. Hu, F.-L. Chang, Y.-H. Zhang, L.-B. Chen, C.-T. Yu, and W.-J. Chang, “Design and Implementation of a Next-Generation Hybrid Internet of Vehicles Communication System for Driving Safety.,” JCM, vol. 13, no. 12, pp. 737–742, 2018.

[5] G. A. Lodi, A. Ott, S. A. Cheema, M. Haardt, and T. Freitag, “Power Line Communication in automotive harness on the example of Local Interconnect Network,” in 2016 International Symposium on Power Line Communications and its Applications, ISPLC 2016, 2016, pp. 212–217.

[6] T. Grandjean, A. Barai, E. Hosseinzadeh, Y. Guo, A. McGordon, and J. Marco, “Large format lithium ion pouch cell full thermal characterisation for improved electric vehicle thermal management,” J. Power Sources, vol. 359, pp. 215–225, 2017.

[7] X. Lin, H. E. Perez, J. B. Siegel, and A. G. Stefanopoulou, “Robust Estimation of Battery System Temperature Distribution Under Sparse Sensing and Uncertainty,” IEEE Trans. Control Syst. Technol., pp. 1–13, Jan. 2019.

[8] R. R. Richardson, P. T. Ireland, and D. A. Howey, “Battery internal temperature estimation by combined impedance and surface temperature measurement,” J. Power Sources, vol. 265, pp. 254–261, Nov. 2014.

[9] United Nations Economic Commission for Europe, “Global Technical Regulation on the Electric Vehicle Safety (EVS),” 2018.

[10] S. Bacquet and M. Maman, “Radio frequency communications for smart cells in battery pack for electric vehicle,” in 2014 IEEE International Electric Vehicle Conference, IEVC 2014, 2015.

[11] C. Cano, A. Pittolo, D. Malone, L. Lampe, A. M. Tonello, and A. G. Dabak, “State of the Art in Power Line Communications: From the Applications to the Medium,” IEEE J. Sel. Areas Commun., vol. 34, no. 7, pp. 1935–1952, Jul. 2016.

[12] T. Muneer, R. Milligan, I. Smith, A. Doyle, M. Pozuelo, and M. Knez, “Energetic, environmental and economic performance of electric vehicles: Experimental evaluation,” Transp. Res. Part D Transp. Environ., vol. 35, pp. 40–61, Mar. 2015.

[13] Yamar Electronics Ltd., “SIG60 Datasheet.” [Online]. Available: https://www.yamar.com/.

[14] L. Pantoli, M. Muttillo, V. Stornelli, G. Ferri, and T. Gabriele, “A low cost flexible power line communication system,” in Lecture Notes in Electrical Engineering, vol. 431, Springer Verlag, 2018, pp. 413–420.

[15] J. B. Robinson et al., “Non-uniform temperature distribution in Li-ion batteries during discharge - A combined thermal imaging, X-ray micro-tomography and electrochemical impedance approach,” J. Power Sources, vol. 252, pp. 51–57, Apr. 2014.

[16] Z. Wang, J. Ma, and L. Zhang, “Finite Element Thermal Model and Simulation for a Cylindrical Li-Ion Battery,” IEEE Access, vol. 5, pp. 15372–15379, Jul. 2017.